Supplementary Information for

Ruthenium Complex Bearing Pyrrolbipyridine and Dimethyl Sulfoxide ligands: Syntheses, Structures, Substitution Reactions, and Catalysis Ammonia Oxidation Behavior

Si-Dan Zhong,[a] Shan Zhao,[a] Chen Zhou,[a], Xi Zhang,[a] Zai-Chao Zhang,[b] Piao He,[a] and Xiao-Yi Yi*[a]

[a] College of Chemistry and Chemical Engineering, Hunan Provincial Key Laboratory of Chemical PowerSources, Central South University, Changsha, Hunan 410083, P. R. China.
[b] Jiangsu Key Laboratory for the Chemistry of Low-Dimensional Materials, School of Chemistry and Chemical Engineering, Huaiyin Normal University, Huai'an, Jiangsu 223300, P. R. China.

* Corresponding authors: Fax: 86 731 888716; Tel: 86 731 88879616;
E-mail address: xyyi@csu.edu.cn

1. ^{1}H NMR, ^{13}C NMR, IR, ESI-MS, UV and Elemental analysis

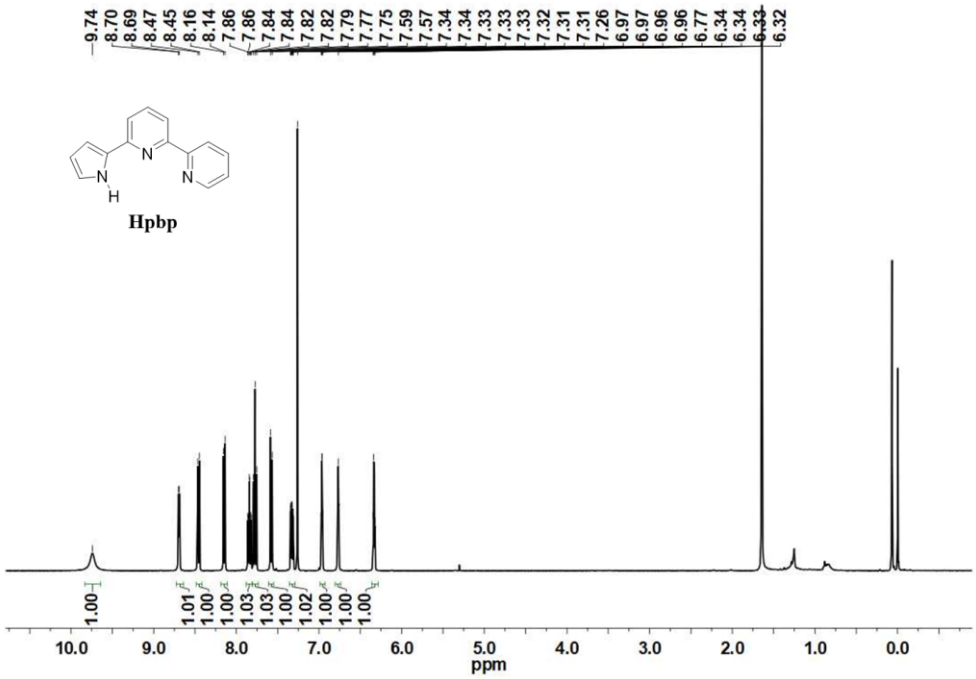

Fig. S1 | ^{1}H NMR ($CDCl_3$) spectrum of 6-(1H-pyrrol-2-yl)-2,2'-bipyridine (**Hpbp**).

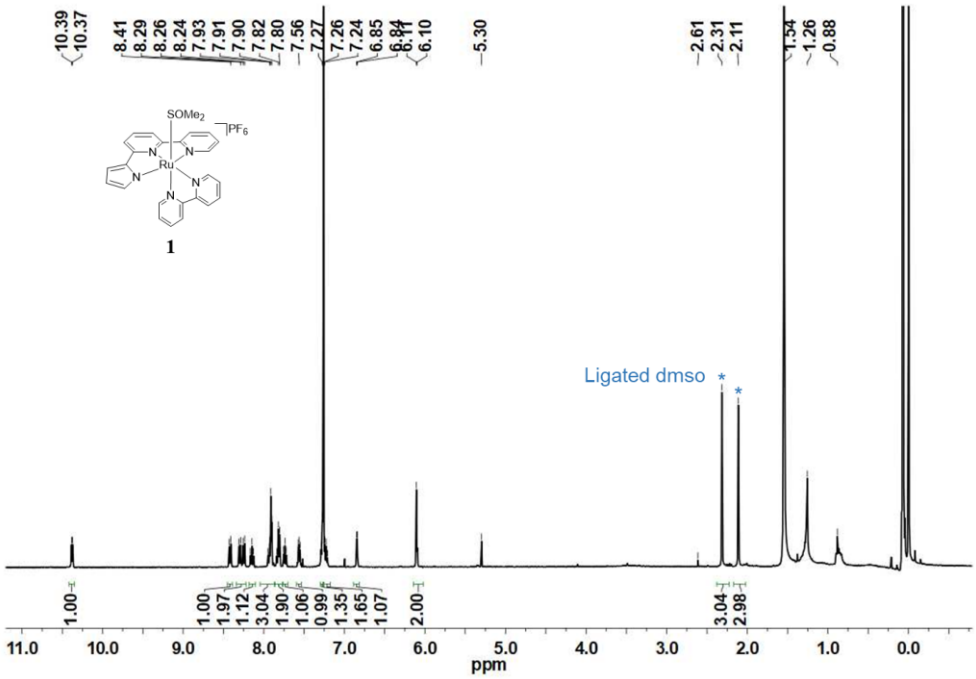

Fig. S2 | ^{1}H NMR ($CDCl_3$) spectrum of **1**.

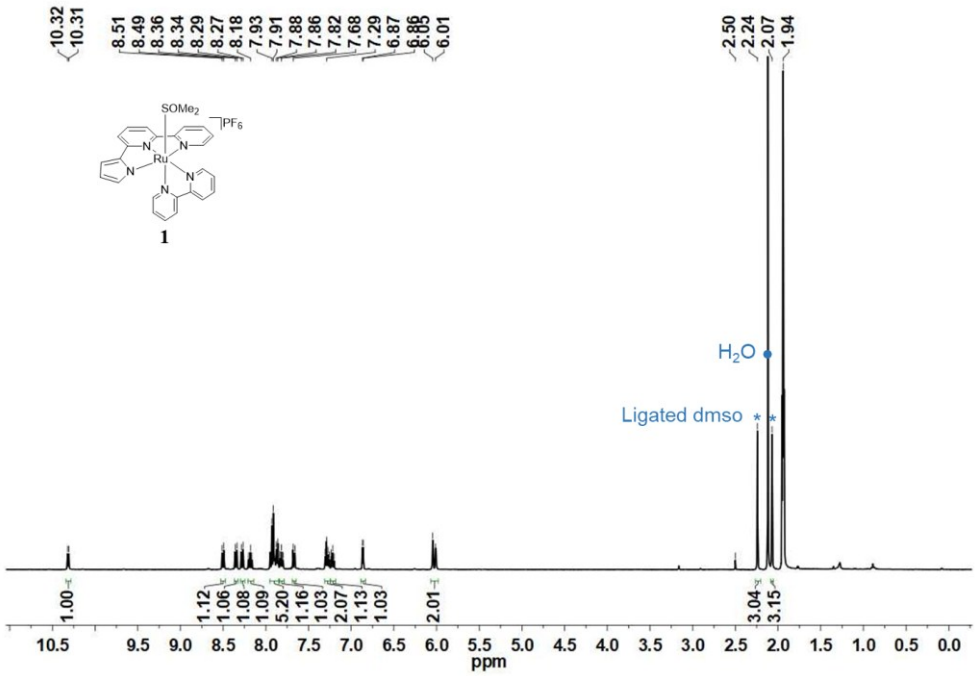

Fig. S3 | ^{1}H NMR (CD_3CN) spectrum of **1**.

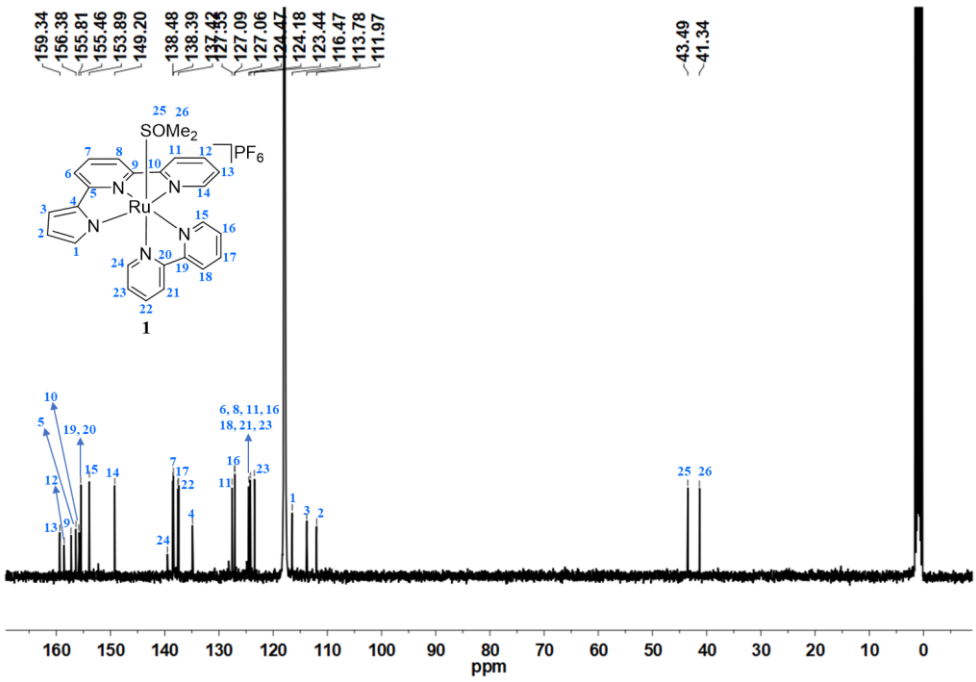

Fig. S4 | ^{13}C NMR (CD_3CN) spectrum of **1**.

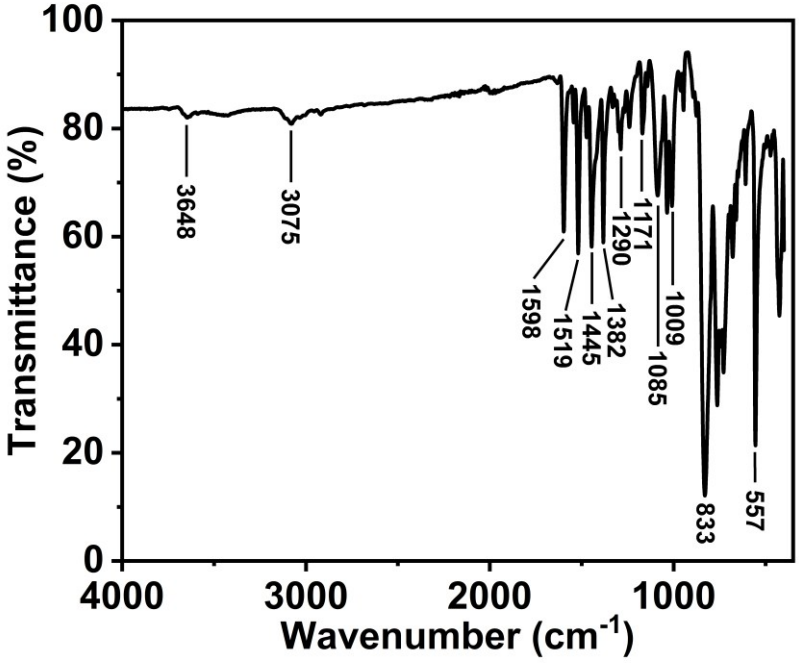

Fig. S5 | IR spectrum of **1**.

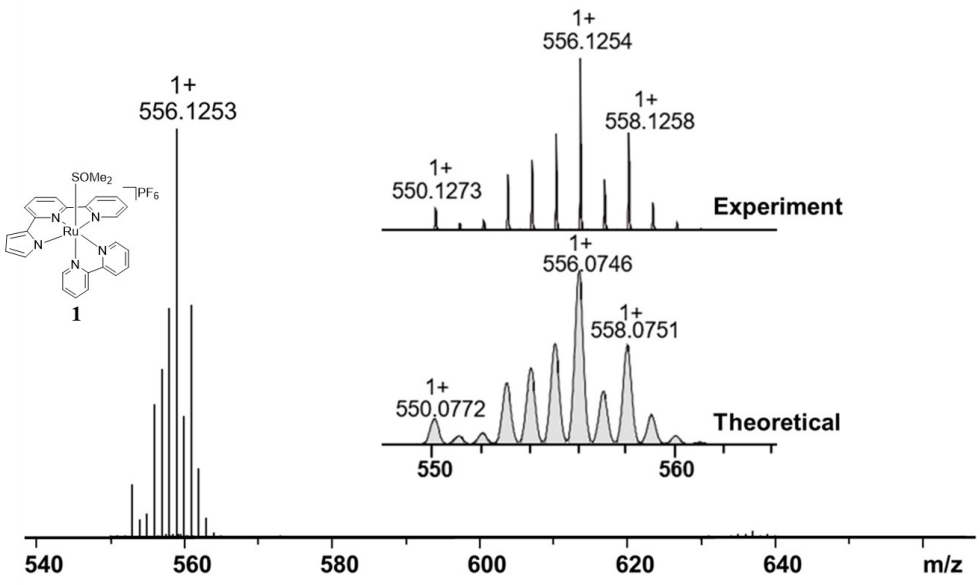

Fig. S6 | ESI-MS spectrum of **1**.

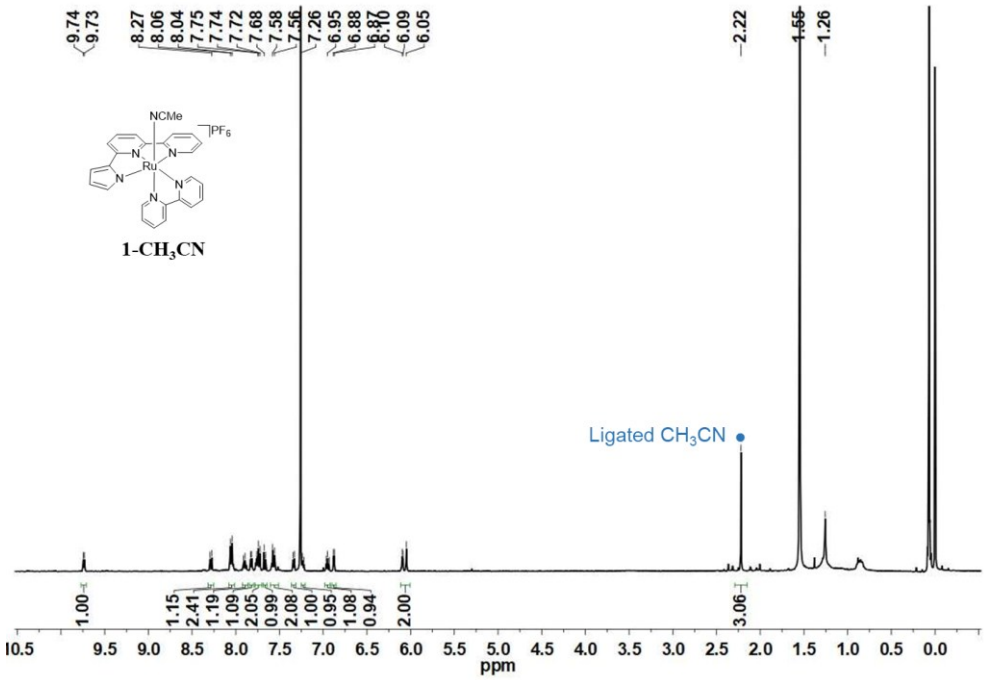

Fig. S7 | ^{1}H NMR ($CDCl_3$) spectrum of **1-CH$_3$CN**.

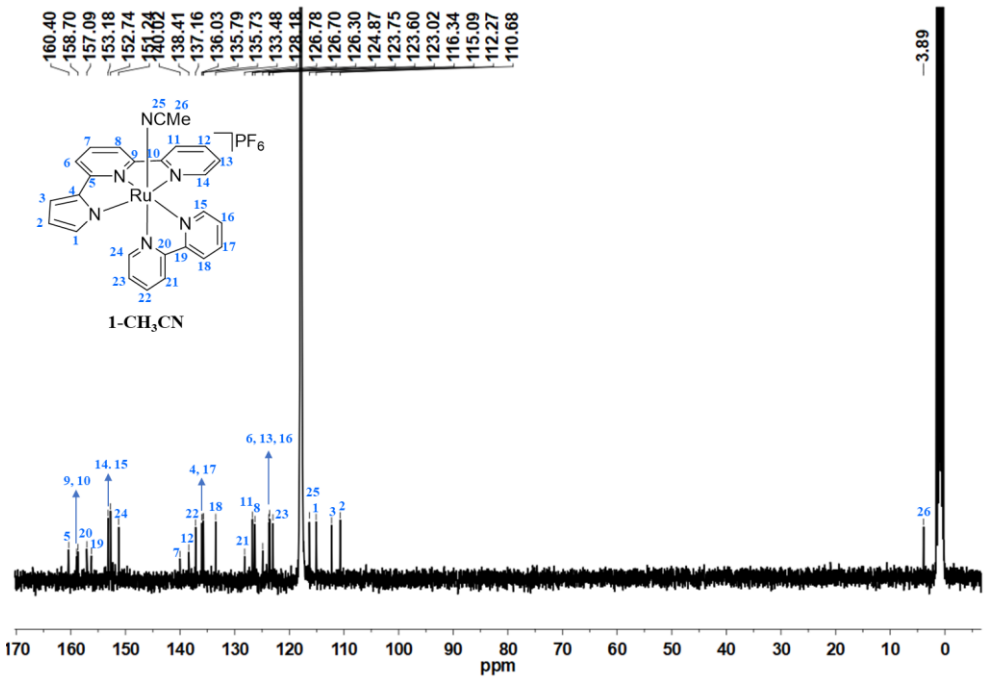

Fig. S8 | ^{13}C NMR (CD_3CN) spectrum of **1-CH$_3$CN**.

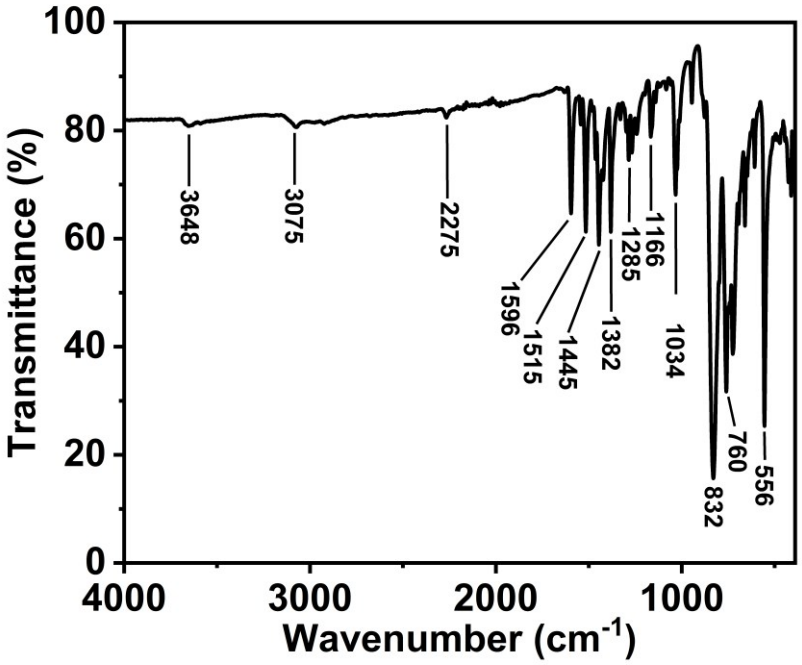

Fig. S9 | IR spectrum of **1-CH_3CN**.

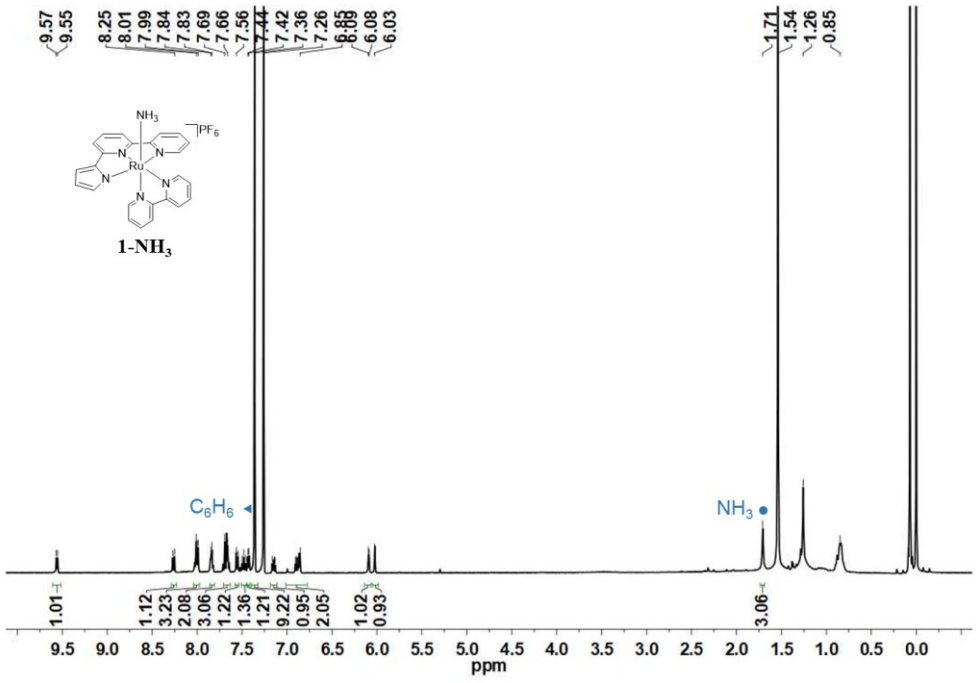

Fig. S10 | ^{1}H NMR ($CDCl_3$) spectrum of **1-NH_3** (signal at δ 7.36 ppm due to the co-crystallized benzene).

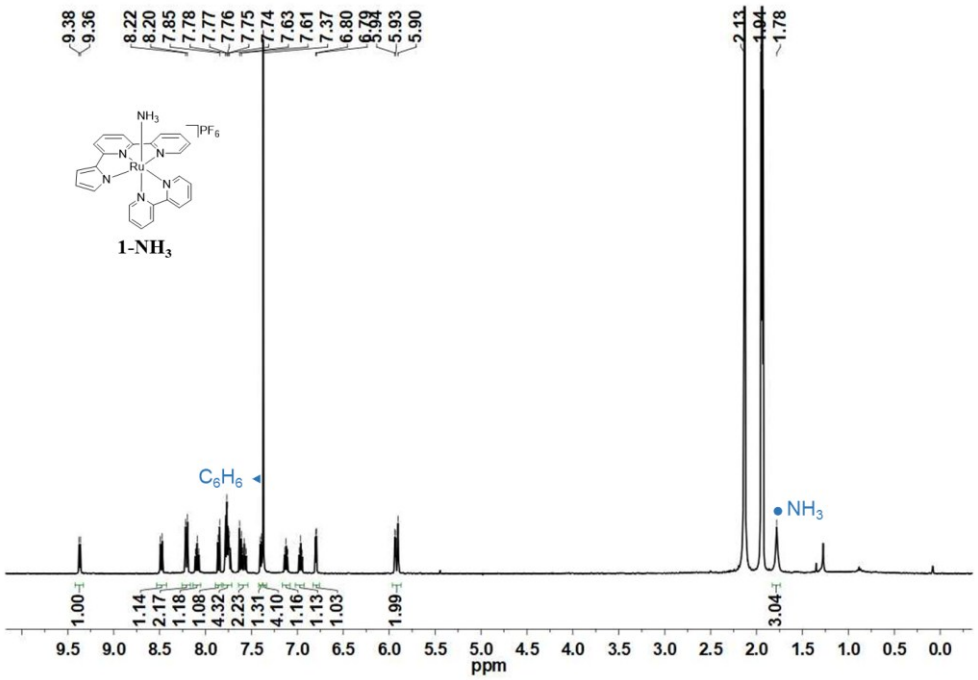

Fig. S11 | ^{1}H NMR (CD_3CN) spectrum of **1-NH$_3$** (signal at δ 7.37 ppm due to the co-crystallized benzene).

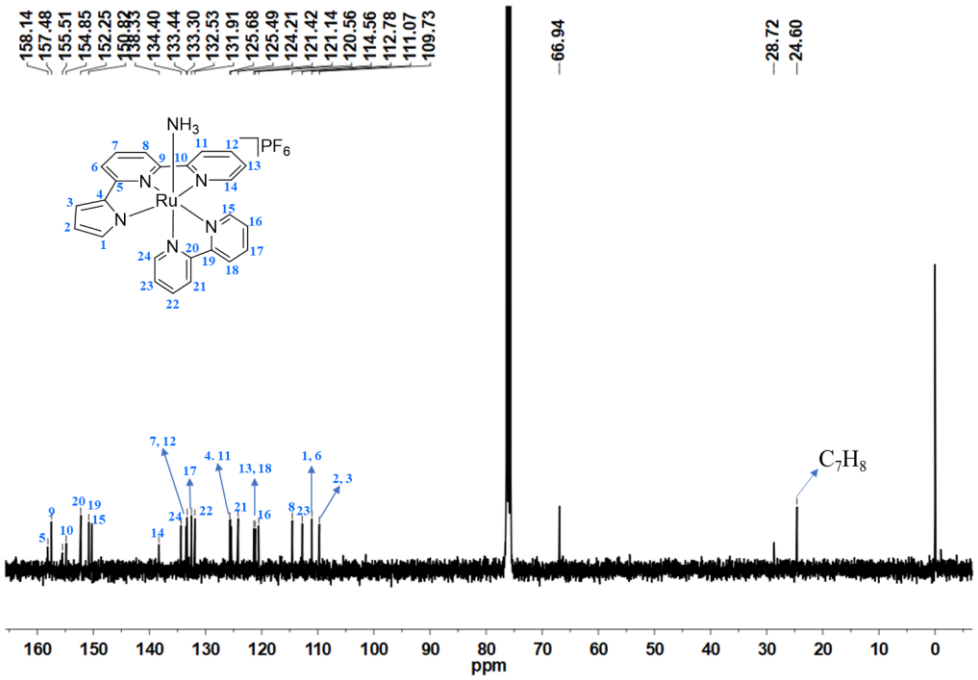

Fig. S12 | ^{13}C NMR ($CDCl_3$) spectrum of **1-NH$_3$**.

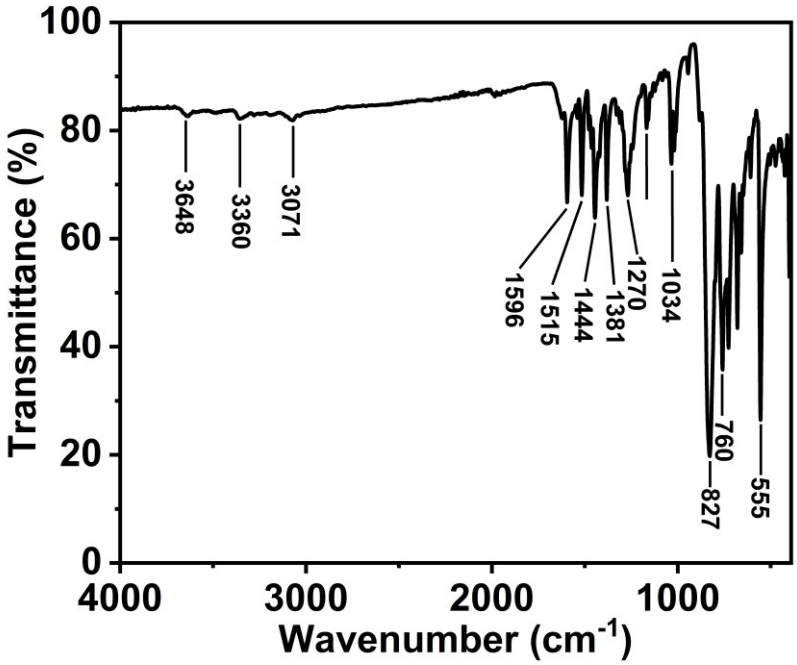

Fig. S13 | IR spectrum of **1-NH$_3$**.

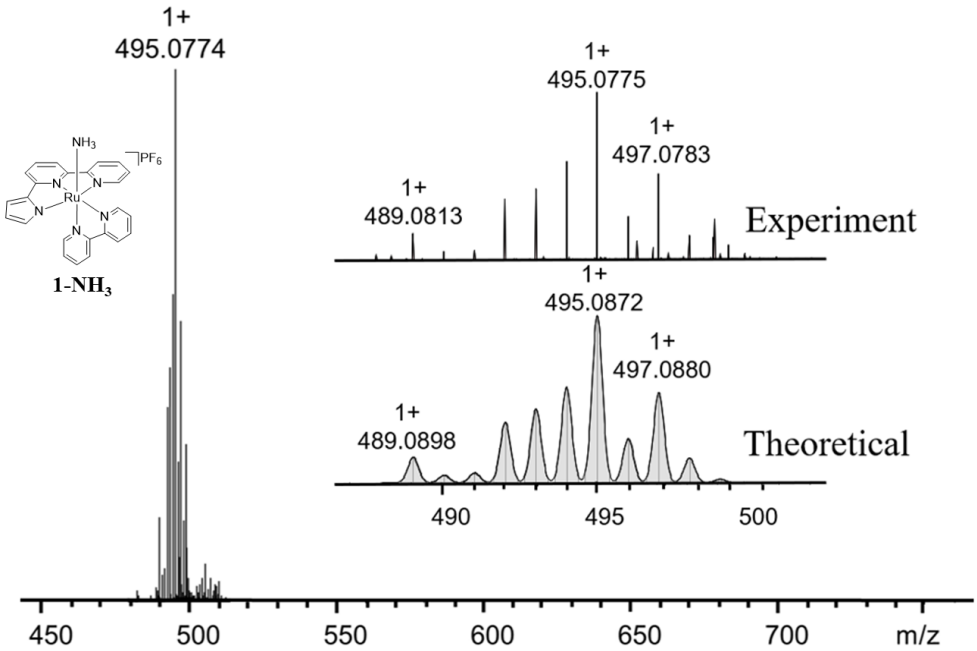

Fig. S14 | ESI-MS spectrum of **1-NH$_3$**.

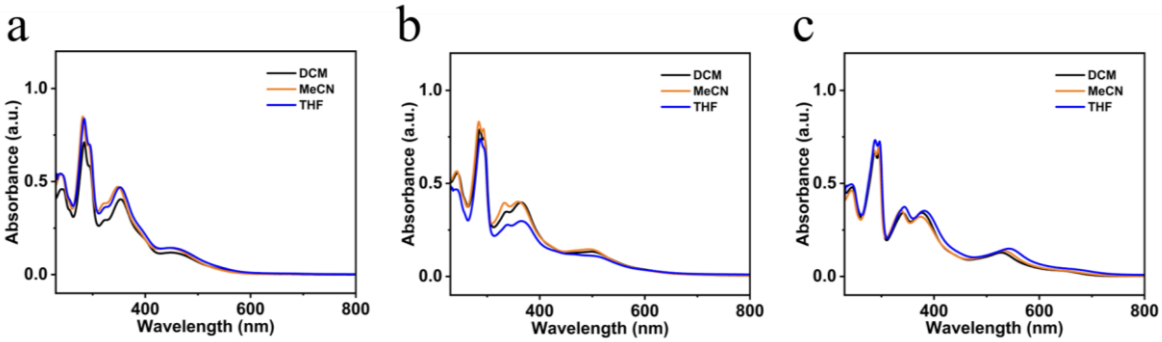

Fig. S15 | The UV-vis absorption spectra of a) **1**, b) **1-CH$_3$CN** and c) **1-NH$_3$** in DCM, CH$_3$CN or THF solvent.

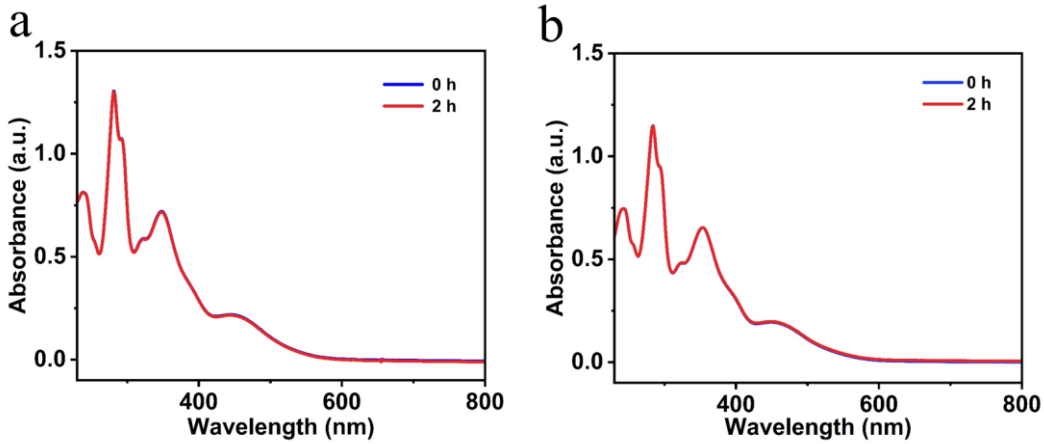

Fig. S16 | a) The UV-vis spectra change for complex **1** (0.015 mM) into **1-CH$_3$CN** in CH$_3$CN solvent in natural light (almost no change after 2 h). b) The UV-vis spectra change for complex **1** (0.015 mM) into **1-NH$_3$** in CH$_2$Cl$_2$ solvent with 0.2 M NH$_3$ in natural light (almost no change after 2 h) .

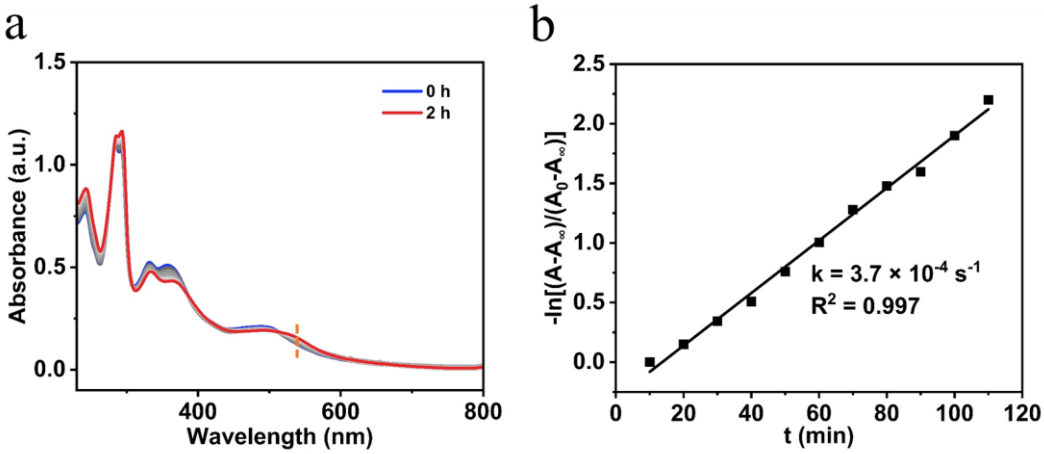

Fig. S17 | a) The UV-vis spectra change for complex **1-CH$_3$CN** (0.015 mM) into **1-NH$_3$** in CH$_2$Cl$_2$ solvent with 0.2 M NH$_3$ in natural light. b) The reaction rate is 3.7×10^{-4} s^{-1}.

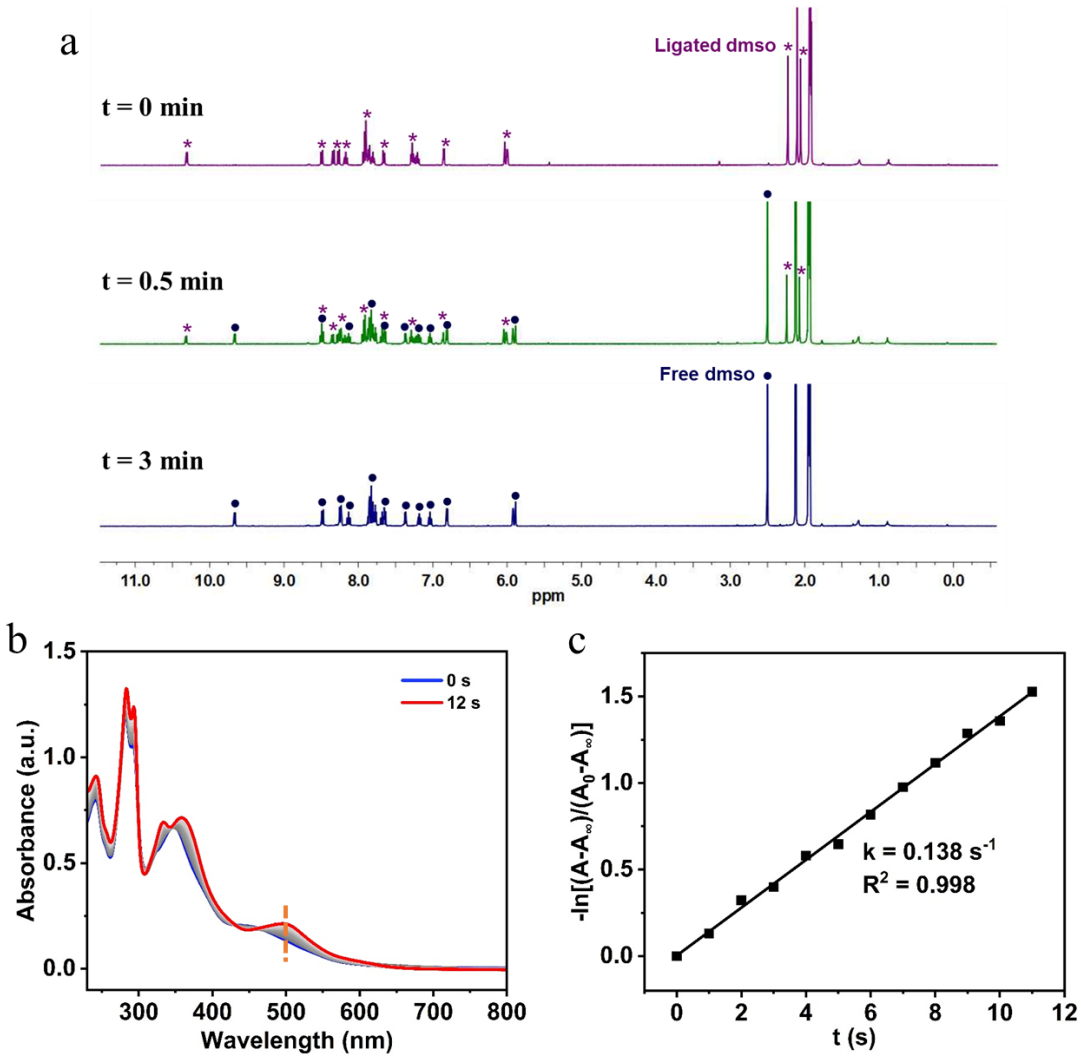

Fig. S18 | a) The ^{1}H NMR (CD_3CN) monitoring experiment of complex **1** (labeled with *) into **1-CH_3CN** (labeled with •) upon irradiation of 300 W Xe lamp. b) The UV-vis spectra change for complex **1** (0.015 mM) into **1-CH_3CN** in CH_3CN solvent with 0.2 M NH_3 upon irradiation of 300 W Xe lamp. c) The reaction rate is 0.138 s^{-1}.

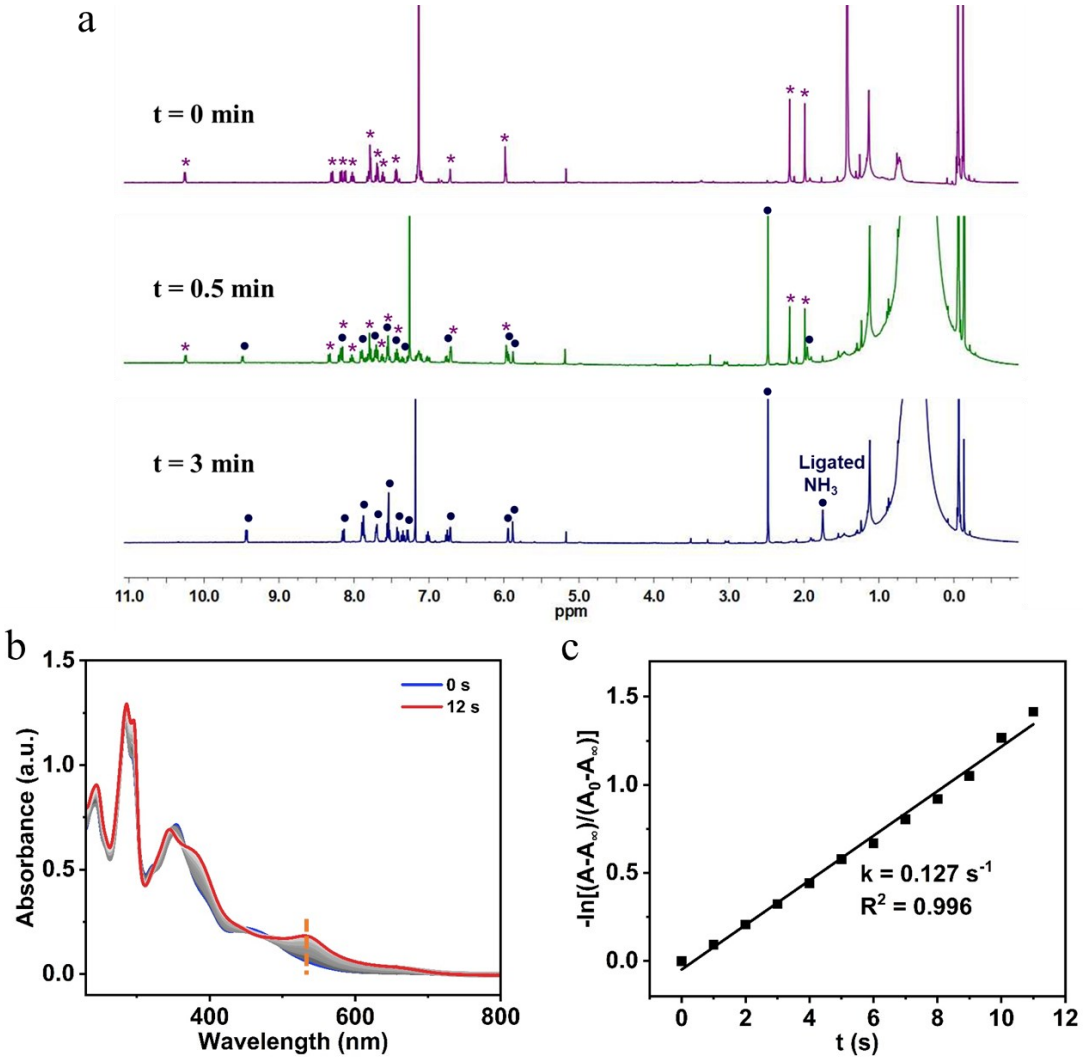

Fig. S19 | a) The ^{1}H NMR ($CDCl_3$) monitoring experiment of complex **1** (labeled with *) into **1-NH_3** (labeled with •) upon irradiation of 300 W Xe lamp. b) The UV-vis spectra change for complex **1** (0.015 mM) into **1-NH_3** in CH_2Cl_2 solvent with 0.2 M NH_3 upon irradiation of 300 W Xe lamp. c) The reaction rate is 0.127 s^{-1}.

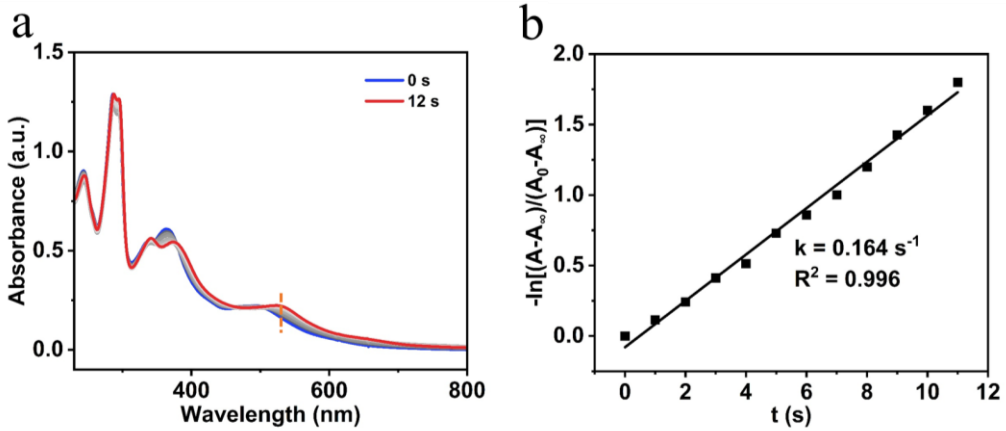

Fig. S20 | a) The UV-vis spectra change for complex **1-CH_3CN** (0.015 mM) into **1-NH_3** in CH_2Cl_2 solvent with 0.2 M NH_3 upon irradiation of 300 W Xe lamp. b) The reaction rate is 0.164 s^{-1}.

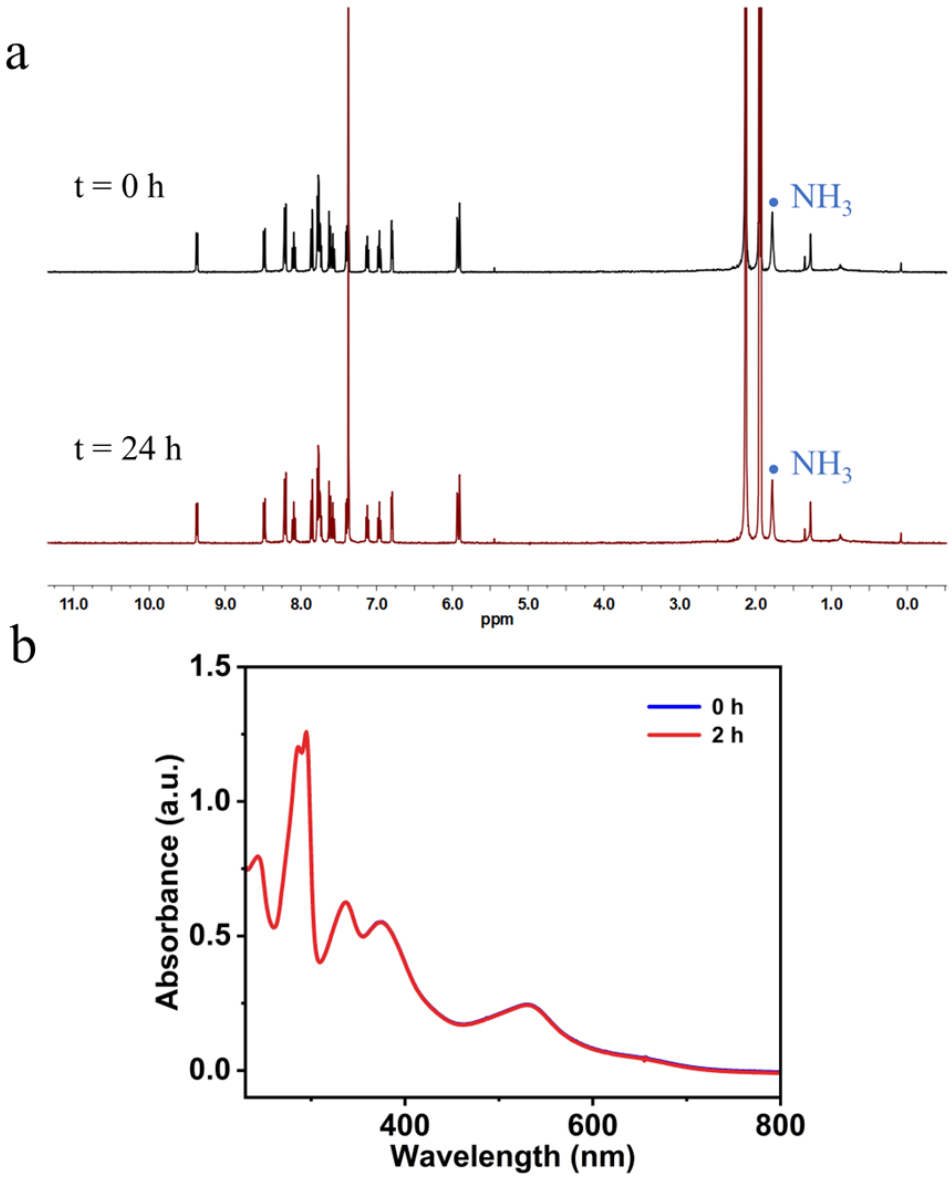

Fig. S21 | a) The ^{1}H NMR (CD_3CN) monitoring experiment of complex **1-NH$_3$** in CD_3CN solvent. b) The UV-vis spectra change for complex **1-NH$_3$** in CH_3CN solvent (almost no change after 2 h).

2. Crystallographic data

Table S1 | Crystallographic data of **1, 1-CH_3CN and 1- NH_3**.

Compound	**1**	**1-CH_3CN**	**1-NH_3**
CCDC	**2428739**	**2428742**	**2428748**
Empirical formula	$C_{26}H_{24}F_6N_5OPRuS$	$C_{26}H_{21}F_6N_6PRu$	$C_{30}H_{27.84}F_6N_6O_{0.42}PRu$
Formula weight	705.10	663.53	725.14
Temperature/K	150(2)	100(2)	153(2)
Crystal system	tetragonal	tetragonal	monoclinic
Space group/number	$P4/n$ (85)	$I4/m$ (87)	$P2_1/c$ (14)
a/Å	16.6299(10)	16.6238(3)	10.9226(4)
b/Å	16.6299(10)	16.6238(3)	25.8025(10)
c/Å	48.630(6)	39.8892(19)	10.5737(4)
α/deg	90	90	90
β/deg	90	90	102.664(4)
γ/deg	90	90	90
Volume/(Å^3)	13449(2)	11023.4(7)	2907.5(2)
Z	8	16	4
ρ_{calc}/(gcm^{-3})	0.696	1.599	1.657
μ/(mm^{-1})	0.318	0.695	0.668
F/000	2836	5312	1465
Reflections collected	98648	31805	21127
Independent reflections	11885	6105	6314
R_{int}	0.1426	0.0873	0.0455
R_{sigma}	0.0988	0.0791	0.0503
Data/Restraints/Parameters	11885/1289/577	6105/4277/752	6314/6/416
Goodness-of-fit on F^2	0.995	1.198	1.015
Final R indexes	R_1 = 0.0742	R_1 = 0.1100	R_1 = 0.0352
[$I \geq 2\sigma(I)$]	wR_2 = 0.1831	wR_2 = 0.2694	wR_2 = 0.0825
Final R indexes	R_1 = 0.1120	R_1 = 0.1637	R_1 = 0.0571
[all data]	wR_2 = 0.2019	wR_2 = 0.2949	wR_2 = 0.0909

[a]GooF = $[\Sigma w(|F_o| - |F_c|)^2/(N_{obs} - N_{param})]^{½}$.

[b]$R_1 = \Sigma||F_o|-|F_c||/\Sigma|F_o|$. [c]$wR_2$ $[(\Sigma w|F_o| - |F_c|)^2/\Sigma w^2|F_o|^2]^{½}$.

Table S2 | Bond lengths (Å) and angles (°) of **1, 1-CH_3CN and 1- NH_3**.

Compound	**1**	**1-CH_3CN**	**1-NH_3**
CCDC	**2428739**	**2428742**	**2428748**
	Bond lengths/Å		
Ru1−N1(A)	2.063(4)	2.100(12)	2.057(2)
Ru1−N2(A)	1.979(4)	1.919(12)	1.977(2)
Ru1−N3(A)	2.095(4)	2.057(15)	2.072(2)
Ru1−N4(A)	2.067(4)	1.996(19)	2.072(2)
Ru1−N5(A)	2.108(4)	2.06(2)	2.025(2)
Ru1−N6(S1A)	2.269(17)	2.035(8)	2.135(3)
	Angle/deg		
N1(A)−Ru1−N2(A)	80.58(17)	80.3(5)	79.89(10)
N1(A)−Ru1−N3(A)	159.67(16)	162.0(6)	157.96(10)
N1(A)−Ru1−N4(A)	89.29(15)	92.4(9)	99.65(9)
N1(A)−Ru1−N5(A)	95.83(15)	92.9(10)	93.22(10)
N1(A)−Ru1−N6(S1A)	94.3(4)	91.8(4)	84.85(10)
N2(A)−Ru1−N3(A)	79.10(16)	81.9(6)	78.53(9)
N2(A)−Ru1−N4(A)	93.39(16)	97.9(8)	174.10(9)
N2(A)−Ru1−N5(A)	170.70(16)	172.0(8)	95.63(9)
N2(A)−Ru1−N6(S1A)	88.9(4)	87.5(4)	89.01(10)
N3(A)−Ru1−N4(A)	91.23(15)	92.7(10)	102.27(9)
N3(A)−Ru1−N5(A)	104.15(14)	105.0(10)	93.28(9)
N3(A)−Ru1−N6(S1A)	86.0(5)	84.7(6)	90.34(9)
N4(A)−Ru1−N5(A)	77.92(15)	78.0(10)	78.51(9)
N4(A)−Ru1−N6(S1A)	176.1(4)	173.6(8)	96.81(9)
N5(A)−Ru1−N6(S1A)	100.0(4)	97.0(7)	174.60(9)

3. Electrochemical studies

CV

The typical sealed three-electrode cell was employed, including an $Ag/AgNO_3$ in 0.1 M $AgNO_3$ acetonitrile solution, a Pt wire, and a glassy carbon electrode (GCE), which were used as the reference electrode, the counter electrode, and the working electrode, respectively.

In acetonitrile solution, the peak potential of ferrocene relative to $Ag/AgNO_3$ in cyclic voltammetry chronoamperometry test is 0.05 V. In dichloromethane solution, the peak potential of ferrocene relative to $Ag/AgNO_3$ in cyclic voltammetry chronoamperometry test is 0.105 V.

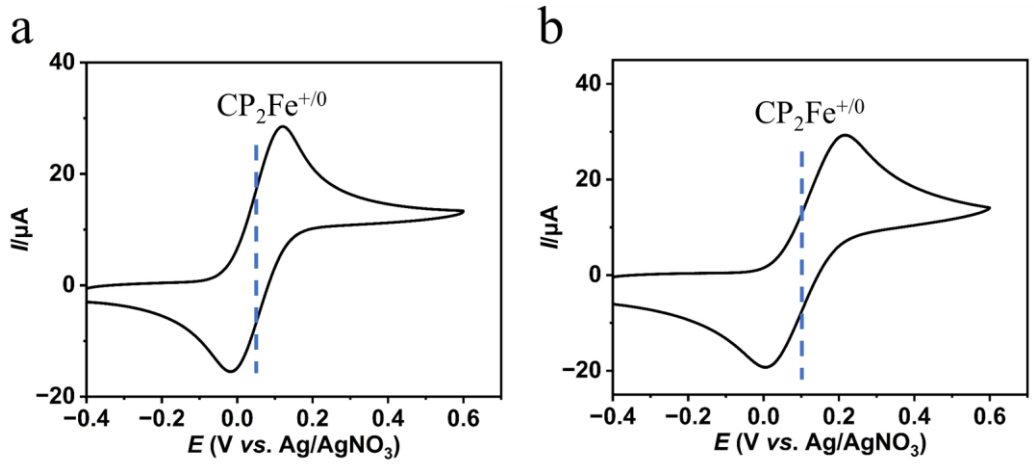

Fig. S22 | The CV of ferrocene as internal standard in a) CH_3CN or b) CH_2Cl_2 solution with scan rate at 100 mV s^{-1}.

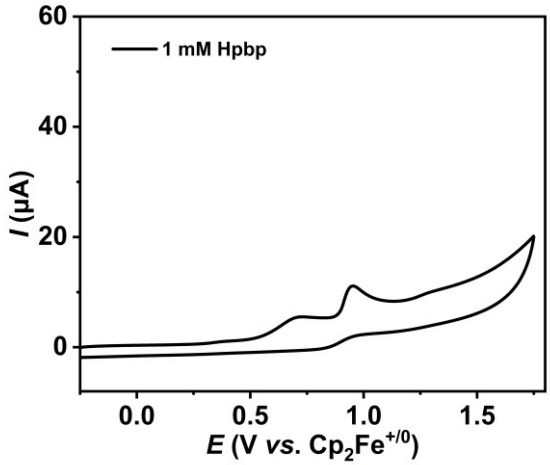

Fig. S23 | The CV of 1mM Hpbp in CH_3CN solution with scan rate at 100 mV s^{-1}.

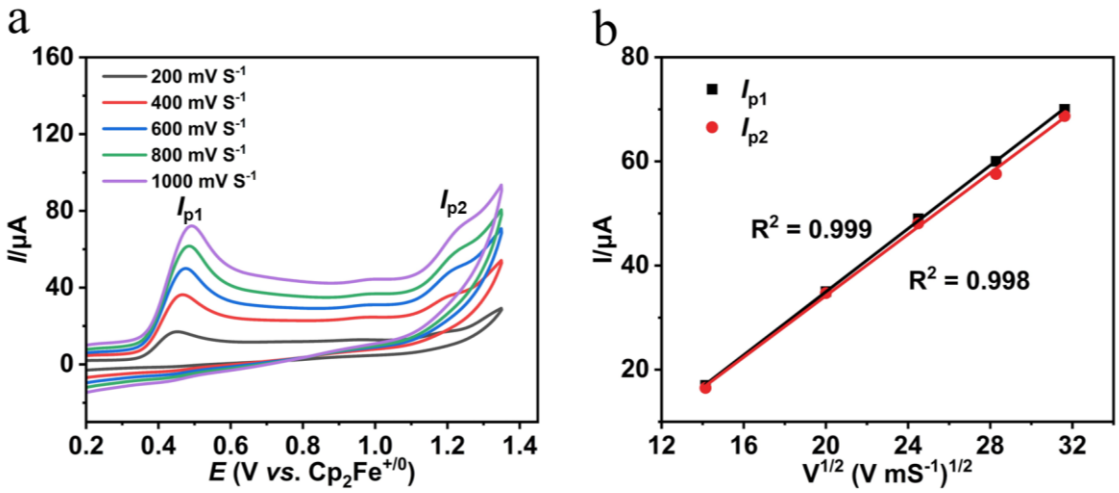

Fig. S24 | CVs of 1 mM complex of a) **1** solution in CH_3CN solution with scan rate at 200, 400, 600, 800, 1000 mV s^{-1} and b) plot of I_p vs. $v^{1/2}$.

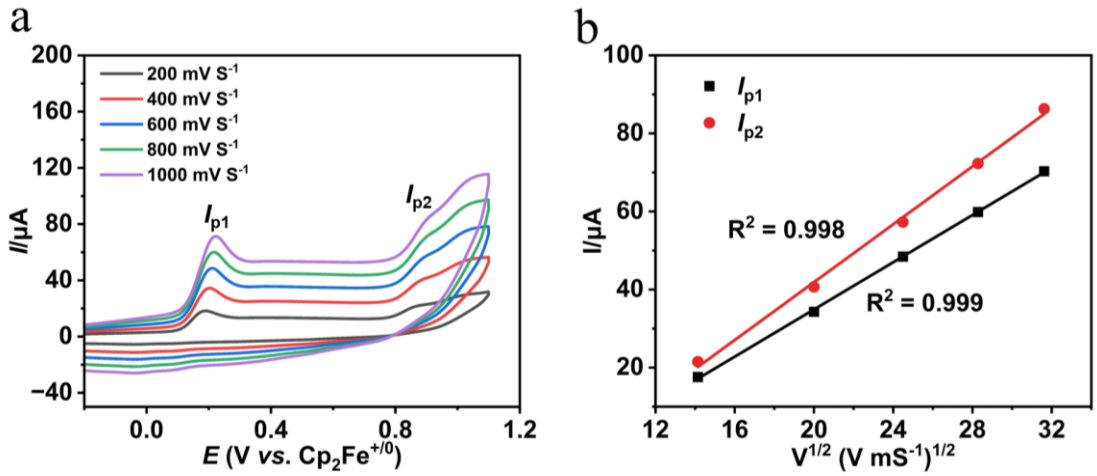

Fig. S25 | CVs of 1 mM complex of a) **1-CH_3CN** solution in CH_3CN solution with scan rate at 200, 400, 600, 800, 1000 mV s^{-1} and b) plot of I_p vs. $v^{1/2}$.

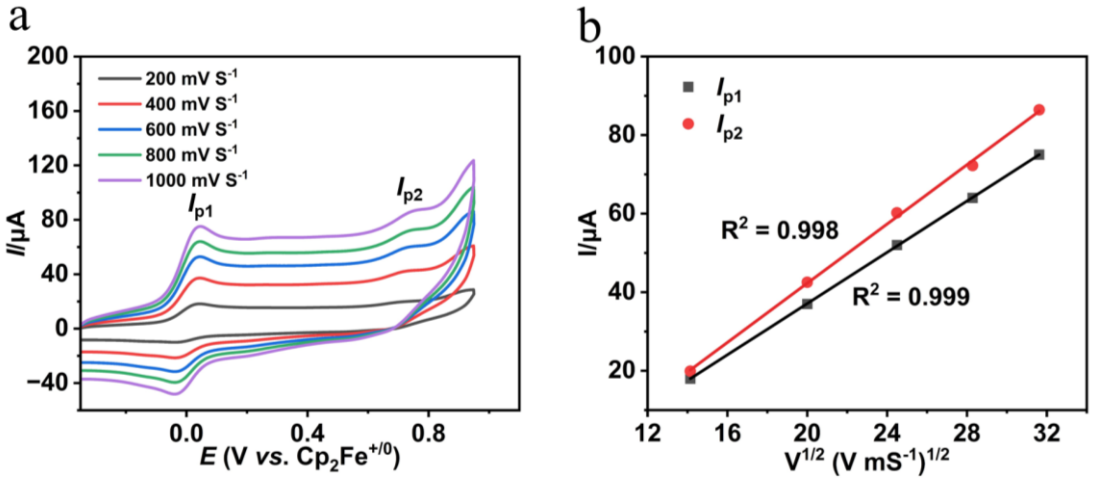

Fig. S26 | CVs of 1 mM complex of a) **1-NH_3** solution in CH_3CN solution with scan rate at 200, 400, 600, 800, 1000 mV s^{-1} and b) plot of I_p vs. $v^{1/2}$.

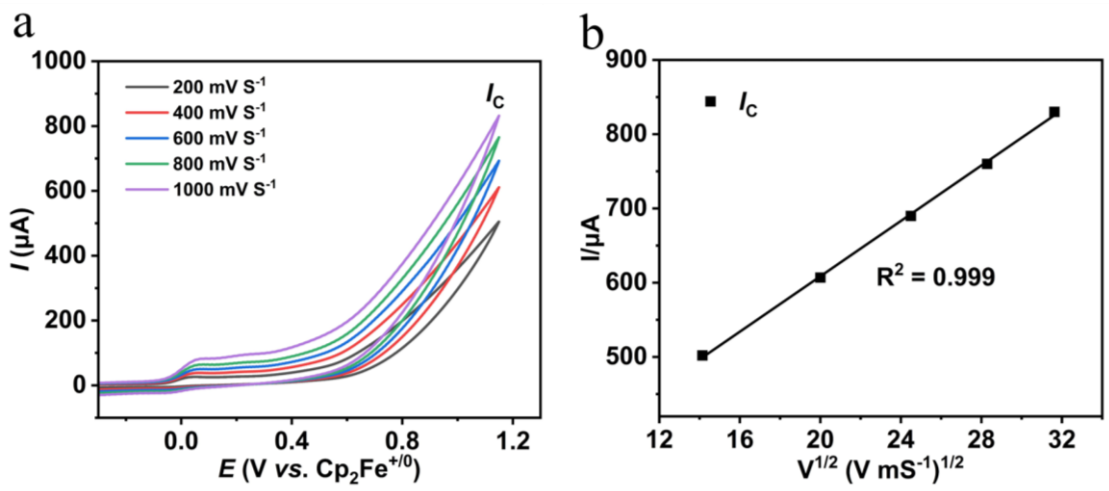

Fig. S27 | a) CVs of 1 mM **1-NH$_3$** in presence of 0.20 M NH_3 in CH_3CN solution with scan rate at 200, 400, 600, 800, 1000 mV s^{-1}; b) Plot of I_c vs. $v^{1/2}$.

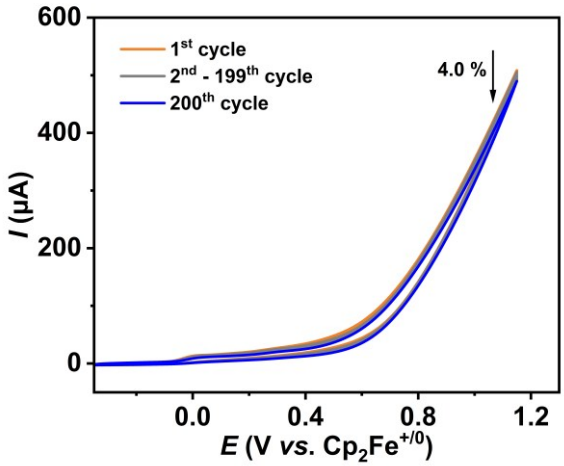

Fig. S28 | Cycling stability of 1 mM **1-NH$_3$** in presence of 0.20 M NH_3 in CH_3CN solution with scan rate at 100 mV s^{-1}.

Table. S3 | Formulas used for the calculation of rate (k) and equilibrium (K) constants.

Equations	Description of parameters
$\frac{I_{c1}}{I_{c2}} = a \cdot \frac{1}{v} + K_{O-S}^{III}$ **(eq. 1)**	I_c = cathodic peak intensity (A) a = RT/nF, with: R = Boltzmann constant (J/(K·mol)) T = temperature (K) n = number of exchanged electrons F = Faraday constant (A·s/mol) v = scan rate (V/s) K = equilibrium constant
$\sqrt{v} = \frac{1}{\frac{0.471}{K_{O-S}^{III}} \cdot \sqrt{\frac{nFl}{RT}}} \cdot \frac{I_d}{I_k} - \frac{1.02}{\frac{0.471}{K_{O-S}^{III}} \cdot \sqrt{\frac{nFl}{RT}}}$ **(eq. 2)**	I_d = diffusional current in the absence of a chemical reaction (= I_{a1}) I_k = measured peak current (= I_{c1}) $l = k_{O-S}^{III} + k_{O-S}^{III}$
$K^{II} = K^{III} + e^{\frac{F}{RT}\cdot(E_{Ru-S}^0 - E_{Ru-O}^0)}$ **(eq. 3)**	E^0 = standard potential
$\ln\left(\frac{I_{a1}}{\sqrt{v}}\right) = k_{O-S}^{II} \cdot \frac{1}{v} + b$ **(eq. 4)**	

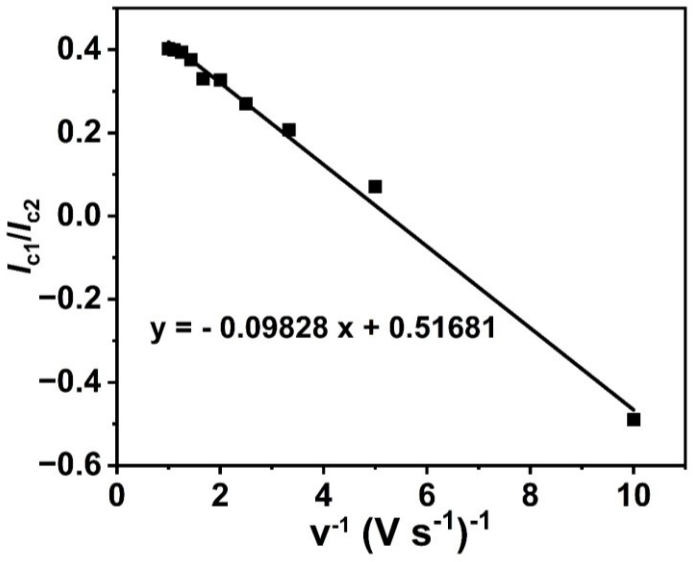

Fig. S29 | Plot of I_{C1}/I_{C2} vs. 1/v to obtain K_{O-S}^{III} for **1**.

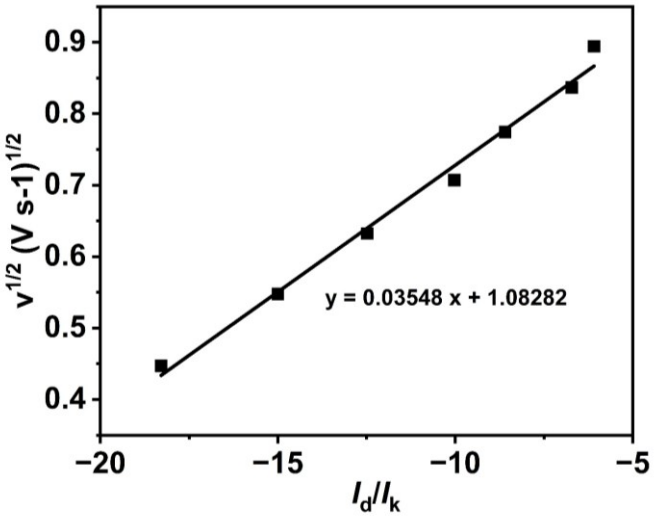

Fig. S30 | Plot of $v^{1/2}$ vs. I_d/I_k to obtain k_{O-S}^{III} for **1**.

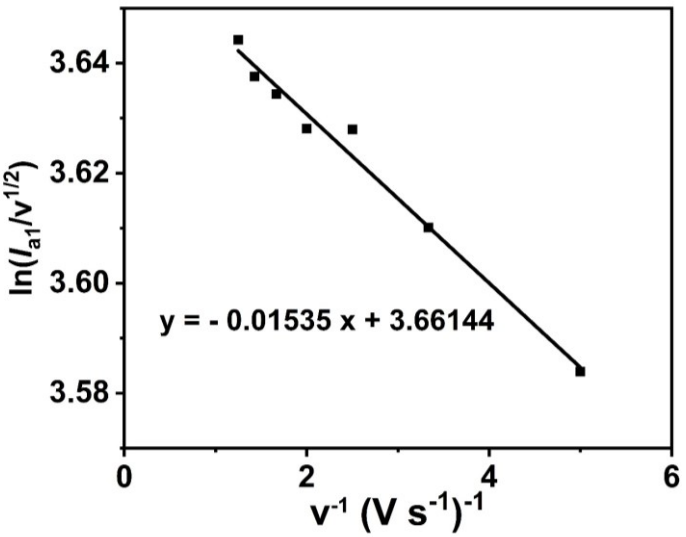

Fig. S31 | Plot of $\ln(I_{a1}/v^{1/2})$ vs. 1/v to obtain k_{O-S}^{II} for **1**.

CPC

Controlled potential coulometry (CPC) measurements.

The carbon cloth (A = 1 cm^2), the platinum plate, and the $Ag/AgNO_3$ in 0.1 M $AgNO_3$ acetonitrile solution were used as the working electrode, counter electrode, and reference electrode, respectively. Unless mentioned otherwise, The CPC experiments were performed in a sealed electrolytic cell (178 mL) under an Ar atmosphere at a given potential (0.1 V or 0.8 V vs. $Cp_2Fe^{+/0}$) with catalyst (0.01 mM), 0.1 M Bu_4NPF_6 as supporting electrolytes and saturated NH_3 solution (2.0 M) in CH_3CN solution.

The determination of turnover number (TON):

$$TON = \frac{n}{n_{cat}} \quad \textbf{(eq. 5)}$$

n is the amount of the products generated by electrocatalytic ammonia oxidation; n_{cat} is the amount of the catalyst involved in electrocatalytic ammonia oxidation.

The determination of faradaic efficiency (FE):

$$FE = \frac{n_{cat}mF}{it} \times 100\% \quad \textbf{(eq. 6)}$$

n_{cat} is the electron transfer number per NH_3 for the ammonia oxidation reaction; m (mol) is the number of moles of the generated product; F is the Faraday constant; i (A) is the current; t (s) is the electrolysis reaction time.

The determination of N_2H_4 selectivity:

$$Selectivity = \frac{n_{N_2H_4}}{n_{N_2H_4} + n_{N_2}} \times 100\% \quad \textbf{(eq. 7)}$$

$n_{N_2H_4}$ and n_{N_2} are the amount of N_2H_4 and N_2 after electrolysis, respectively.

Table S4 | The electrocatalytic performances of background. [a]

Entry	Catalyst	E_{app} [b] (V vs. $Cp_2Fe^{+/0}$)	Time (h)	n_{H2} (μmol)	n_{N2} (μmol)	n_{N2H4} (μmol)
1	-	0.1	24	-	-	-
2	-	0.8	2	104.6	11.2	70.7

[a] conditions: carbon cloth (1 cm^2) as working electrode, platinum plate (1 cm^2) as counter electrode, $AgNO_3/Ag$ in 0.1 M $AgNO_3$ acetonitrile solution as reference electrode, 0.1 M Bu_4NPF_6 as supporting electrolytes, $[NH_3]$ = 2 M, [b] E_{app} vs. $Cp_2Fe^{+/0}$.

Gas Chromatography (GC) methods.

Gas quantification was performed using a molecular sieve column attached to a thermal conductivity detector. Ar was used as the carrier gas.

The standard curves for H_2, N_2, and O_2 were created by directly injecting different volumes (100, 200, 300, 400, 500 μL) of standard gases. The concentrations of H_2, N_2, and O_2 in the standard gases were 2503.8, 406.3, and 98.8 ppm, respectively.

The standard gas at the headspace of reactor was manually injected to the GC using a gastight syringe (SGE Analytical Science). The linear regression equation of H_2 is y = 260733.9 x – 60.8 with R^2 = 0.998. The linear regression equation of N_2 is y = 47358.1 x + 125.3 with R^2 = 0.993. The linear regression equation of O_2 is y = 58947.4 x + 44.8 with R^2 = 0.963. The GC calibration curves H_2, N_2 and O_2 are shown in Fig. S32.

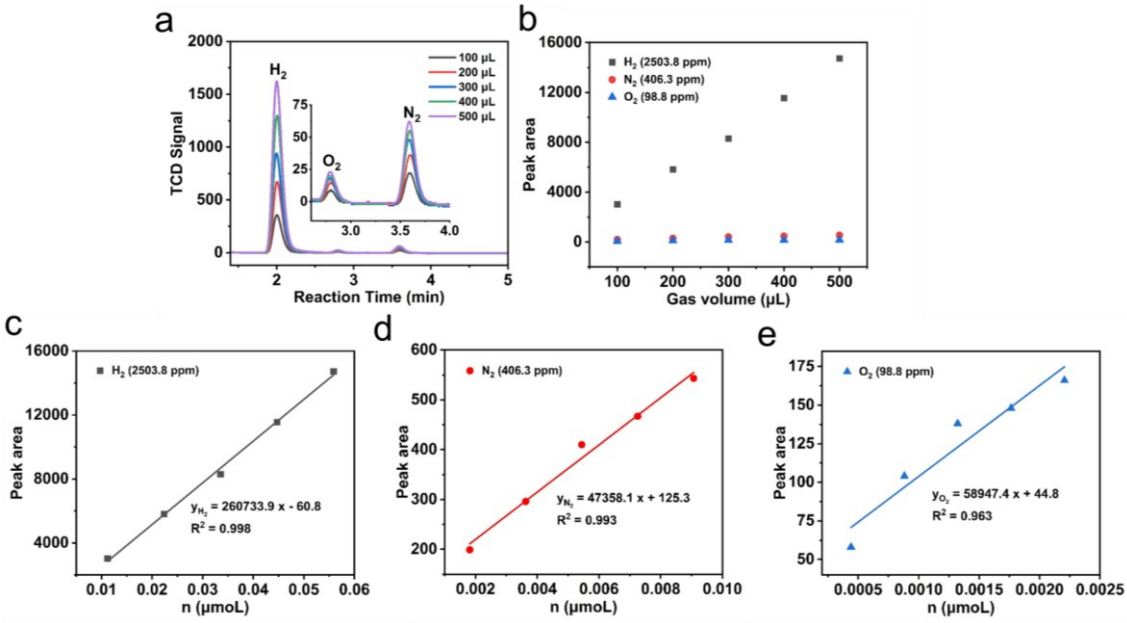

Fig. S32 | Representative a) GC-TCD trace and b) the corresponding peak area of H_2, N_2, and O_2 for standard gases of different volumes (100, 200, 300, 400, 500 μL) and Gas Chromatography calibration lines for c) H_2, d) N_2 and e) O_2.

N_2H_4 Test.

Preparation of hydrazine standard solution (1.00 μg/mL): Weigh 0.0406 g (containing 0.01g N_2H_4) of hydrazine sulfate (N_2H_4•H_2SO_4), dissolve with 1 M HCI solution, transfer quantitatively to a 100 mL volumetric flask, and dilute to the standard line. Transfer 1 mL of the above solution to a 100 mL volumetric flask and dilute with 1 M HCI solution to the standard line to obtain 1.00 ug/mL hydrazine standard solution.

Preparation of color reagent： The color reagent was prepared by weighing 4 g of *p*-$C_9H_{11}NO$ dissolved in 200 mL 95% ethanol and 20 mL 37% HCI.

Calibration curve of hydrazine: Eight 10 mL colorimetric tubes were prepared by adding 0, 0.2, 0.4, 0.8, 1.6, 2.4, 3.2, and 4.0 mL of hydrazine standard solution, followed by 4 mL of color reagent. Each solution was then diluted to the 10 mL mark with deionized water. The concentration of hydrazine in the eight centrifuge tubes is 0, 0.625, 1.25, 2.5, 5.0, 7.5, 10.0, 12.5 μmol/L respectively. After thorough mixing, the solutions were left to stand at room temperature for 1 hour,

protected from light. Absorbance was measured at 458 nm using a cuvette with a 10 mm light path. A concentration-absorbance calibration curve was plotted, with hydrazine content as the abscissa (x-axis) and absorbance as the ordinate (y-axis). The linear regression equation of N_2H_4 is y = 0.06472 x + 0.02566 with R^2 = 0.999. (Fig. S33)

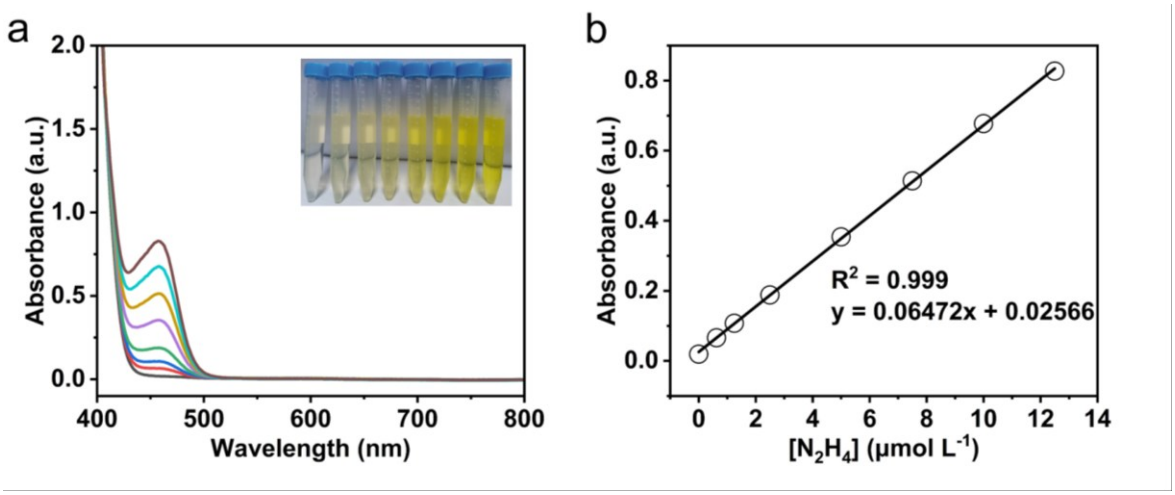

Fig. S33 | Calibration curve used for calculation of N_2H_4 concentrations.

Effect of electrolyte Bu_4NPF_6 on the detection of hydrazine:

a) 0, 7.7 mg of tetrabutylammonium hexafluorophosphate (Bu_4NPF_6) was added into 10 mL colorimetric tubes respectively, 4 mL of color reagent was added to each for color reaction, deionized water was added to dilute to 10 mL (at this time, the concentrations of Bu_4NPF_6 in the centrifugal tubes were 0 mM and 2.0 mM, respectively), and waited for 1 hour to perform UV test. The UV showed that the introduction of the Bu_4NPF_6 did not produce an N_2H_4 signal peak.

b) 0, 7.7 mg of Bu_4NPF_6 was added into 10 mL centrifuge tubes respectively, 2.4 mL of 1 μg L^{-1} N_2H_4 standard solution and 4 mL of color reagent were added for the color reaction, and then deionized water was added to dilute to 10 mL (at this time, the concentrations of Bu_4NPF_6 in the centrifuge tubes were 0 mM and 2.0 mM, respectively; the concentration of N_2H_4 was 7.5 μM) and the UV test was carried out after a 1 hour wait. The UV showed that the introduction of the Bu_4NPF_6 did not produce the N_2H_4 signal peak.

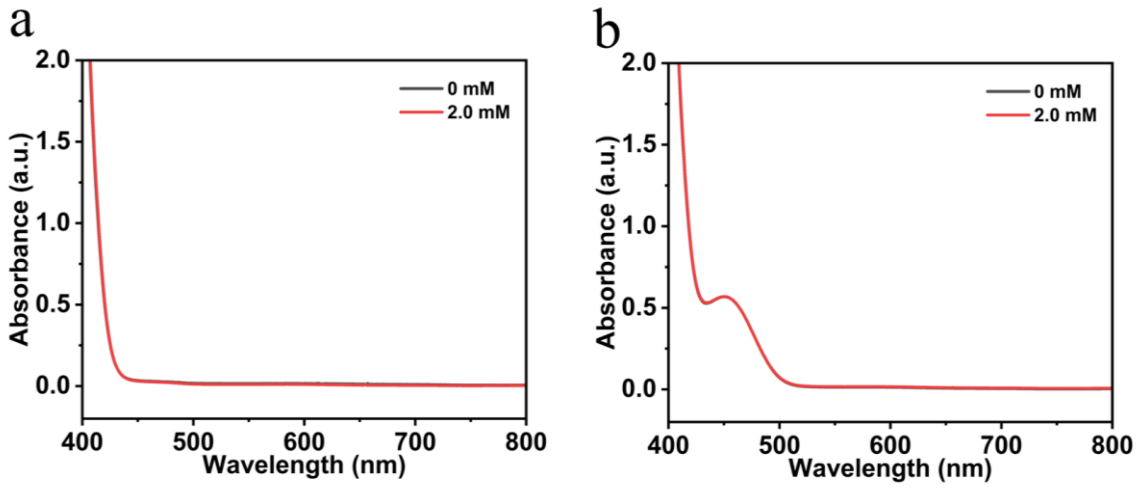

Fig. S34 | The UV-Vis spectrum of Bu_4NPF_6 effect on detection of hydrazine.

NO_2^- Test.

Preparation of nitrite standard solution (20.0 μM): Nitrite standard solutions were prepared by dissolving 69.0 mg (1 mmol) of $NaNO_2$ in 100 mL of deionized water. The resulting 10 mM $NaNO_2$ solution was further diluted with deionized water to give solutions of 20.0 μM.

Preparation of color reagent： Color reagent **A** (1.0 mM) was prepared by dissolving sulfanilamide (17.2 mg, 0.1 mmol) in 5 mL of 37% HCl, then diluting the solution to 100 mL with deionized water. Color reagent **B** (1.0 mM) was prepared by dissolving 1-naphthylamine (14.3 mg, 0.1 mmol) in 5 mL of 37% HCl and then diluting the solution to 100 mL with deionized water. Reagents **A** and **B** were stored in the dark at room temperature.

Calibration curve: For the nitrite standard curve, 0, 2.0, 4.0, 6.0 and 8.0 mL of as-prepared nitrite standard solutions ($NaNO_2$ aqueous solution) were transferred to different colorimetric tubes. Reagent **A** (1 mL) and reagent **B** (1 mL) were added to the colorimetric tubes and diluted to 10 mL. The mixtures were well shaken and allowed to stand for 5 min at room temperature before being analysed by UV–vis spectroscopy with a characteristic absorption band at 518.0 nm.

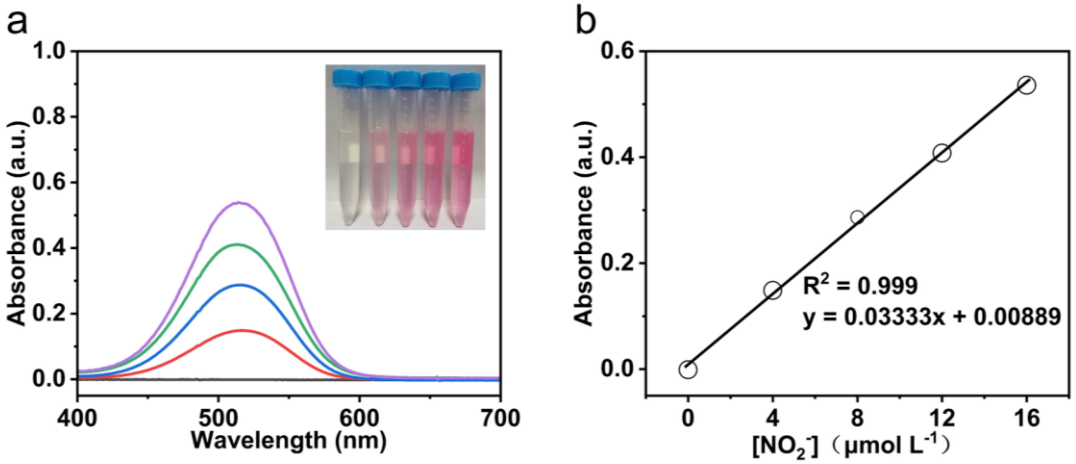

Fig. S35 | Calibration curve used for calculation of NO_2^- concentrations.

NO_3^- Test.

Preparation of nitrite standard solution (2.0 mM): A nitrate standard solution was prepared by dissolving 8.5 mg (0.1 mmol) of $NaNO_3$ in 50 mL of deionized water.

Preparation of color reagent (2.0 mM): An ammonium sulfamate solution (2.0 mM) was prepared by dissolving 22.8 mg (0.2 mmol) of ammonium sulfamate in 5 mL of 37% HCl. This was then diluted to 100 mL with deionized water.

Calibration curve: For the nitrite standard curve, 0, 0.2, 0.4, 0.6, 0.8 and 1 mL of as-prepared nitrate standard solutions ($NaNO_3$ aqueous solutions) were transferred to different colorimetric tubes. Ammonium sulfamate solution (1 mL) was added to the colorimetric tubes and the solutions were diluted to 10 mL. The mixtures were well shaken and allowed to stand for 5 min at room temperature before being analysed by UV–vis spectroscopy with a characteristic absorption band at 219.0 nm.

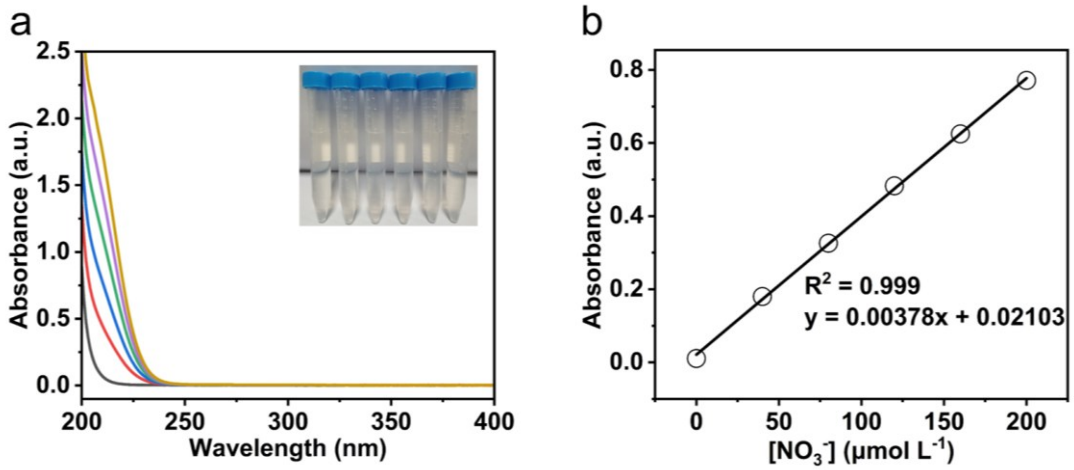

Fig. S36 | Calibration curve used for calculation of NO_3^- concentrations.

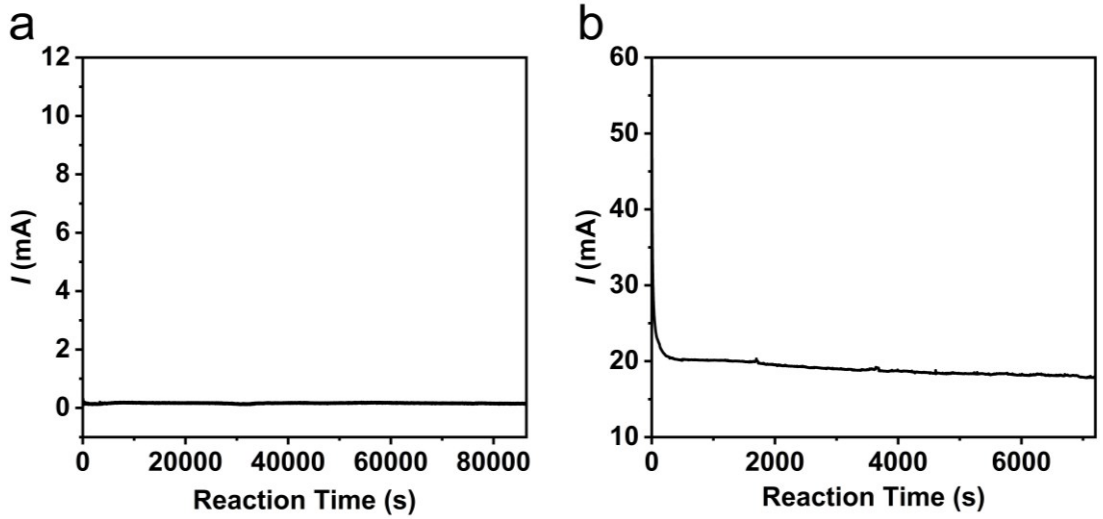

Fig. S37 | CA response recorded from the CPC experiment of NH_3 solution (2.0 M) in CH_3CN solution containing **1-NH₃** (0.01 mM) at an applied potential of (a) 0.1 V, (b) 0.8 V vs. $Cp_2Fe^{+/0}$ in natural light.

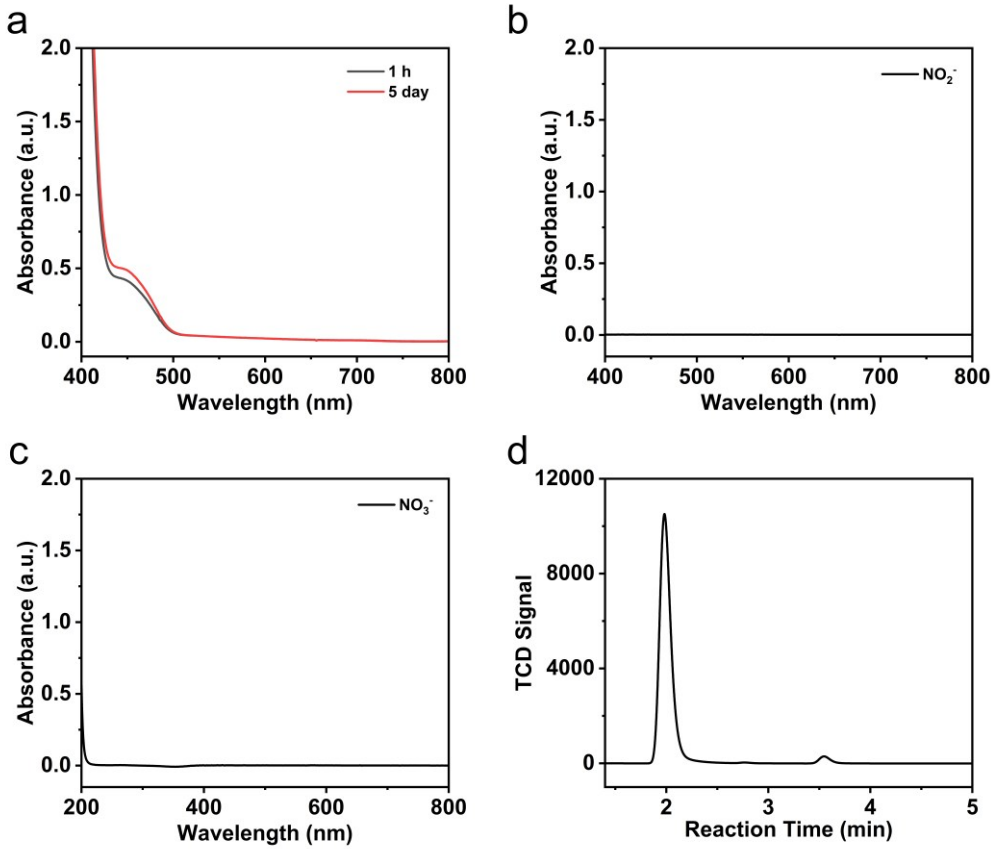

Fig. S38 | Determination of (a) N_2H_4, (b) NO_2^-, (c) NO_3^- in the electrolyte and (d) GC-TCD trace of H_2, O_2 and N_2 after the CPC experiment of NH_3 solution (2.0 M) in CH_3CN solution containing **1-NH₃** (0.01 mM) at an applied potential of 0.8 V vs. $Cp_2Fe^{+/0}$ for 2 h in natural light.

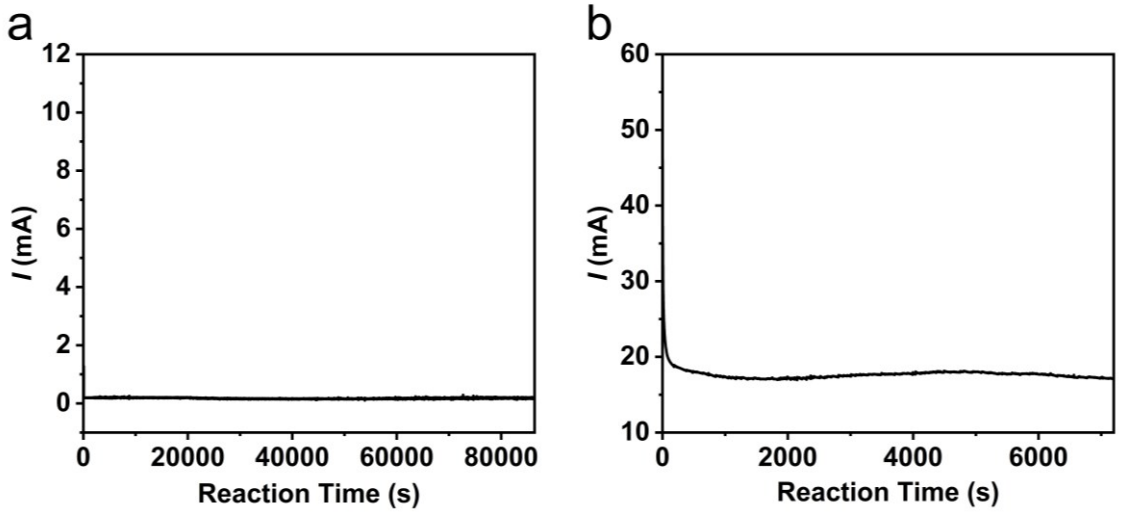

Fig. S39 | CA response recorded from the CPC experiment of NH_3 solution (2.0 M) in CH_3CN solution containing **1-NH₃** (0.01 mM) at an applied potential of (a) 0.1 V, (b) 0.8 V vs. $Cp_2Fe^{+/0}$ in the darkness.

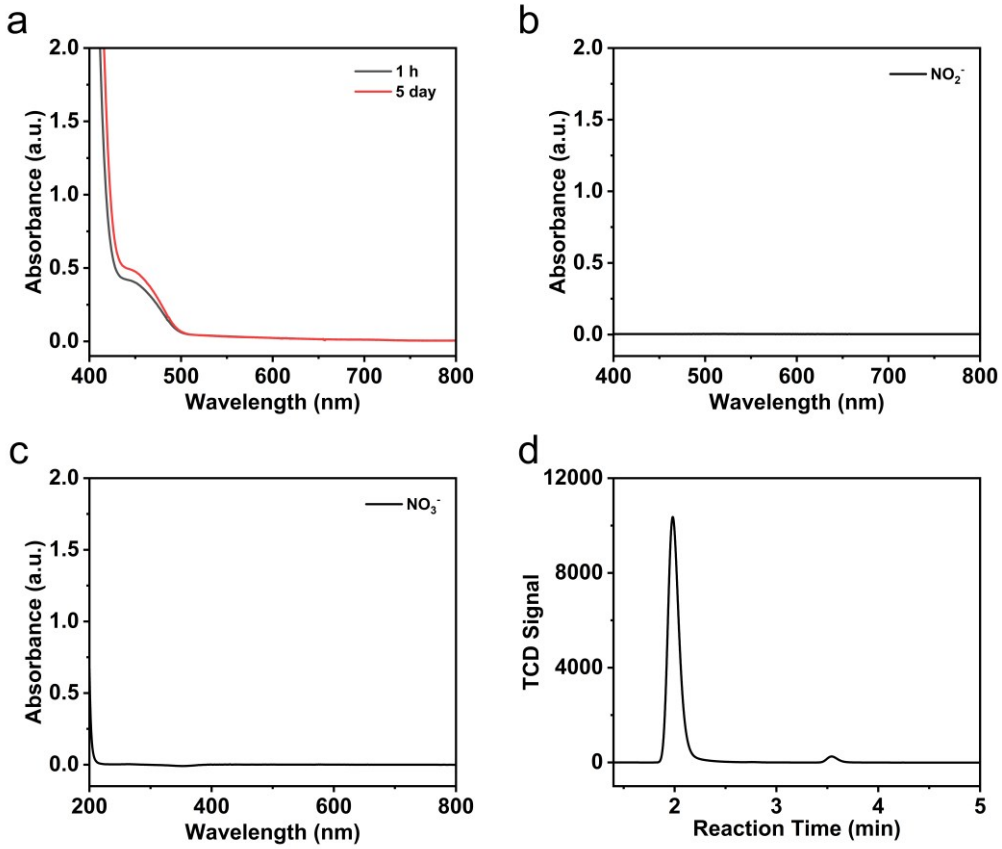

Fig. S40 | Determination of (a) N_2H_4, (b) NO_2^-, (c) NO_3^- in the electrolyte and (d) GC-TCD trace of H_2, O_2 and N_2 after the CPC experiment of NH_3 solution (2.0 M) in CH_3CN solution containing **1-NH₃** (0.01 mM) at an applied potential of 0.8 V vs. $Cp_2Fe^{+/0}$ for 2 h in the darkness.

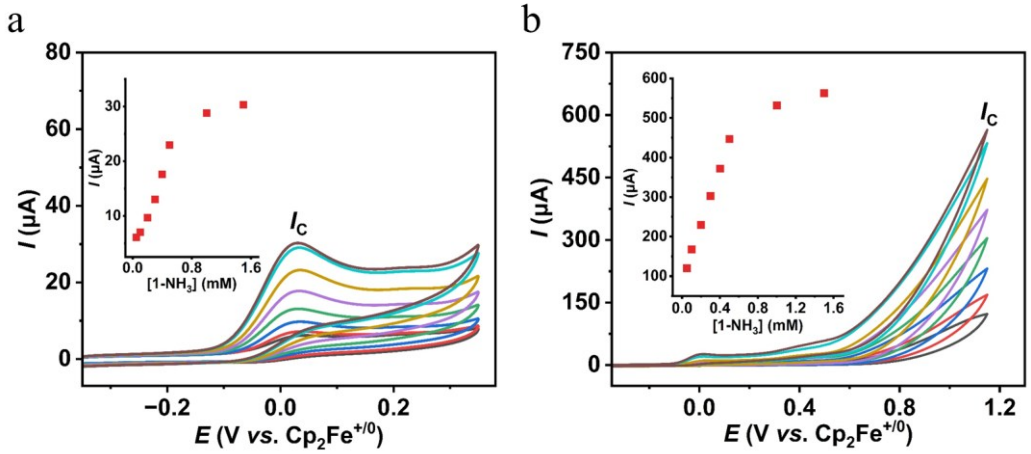

Fig. S41 | The CVs of complex **1-NH$_3$** (0.05, 0.1, 0.2, 0.3, 0.4, 0.5, 1.0, 1.5 mM) at different concentrations in the presence of 0.2 M NH_3 in CH_3CN solution with scan rate at 100 mV s^{-1}.

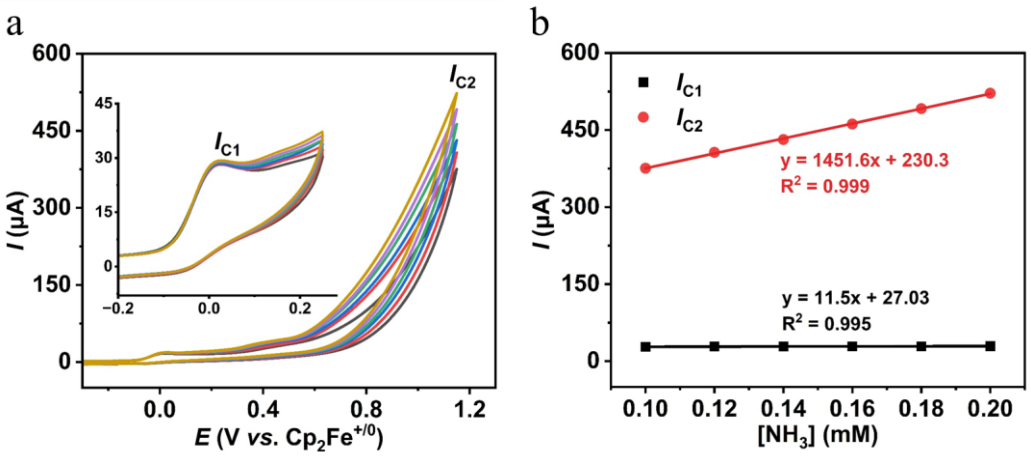

Fig. S42 | a) CVs of 1 mM **1-NH$_3$** in presence of different NH_3 concentrations (0.10, 0.12, 0.14, 0.16, 0.18, 0.20 M) in CH_3CN with scan rate at 100 mV s^{-1}. b) Plot of I_c vs. [NH_3].

DLS and SEM

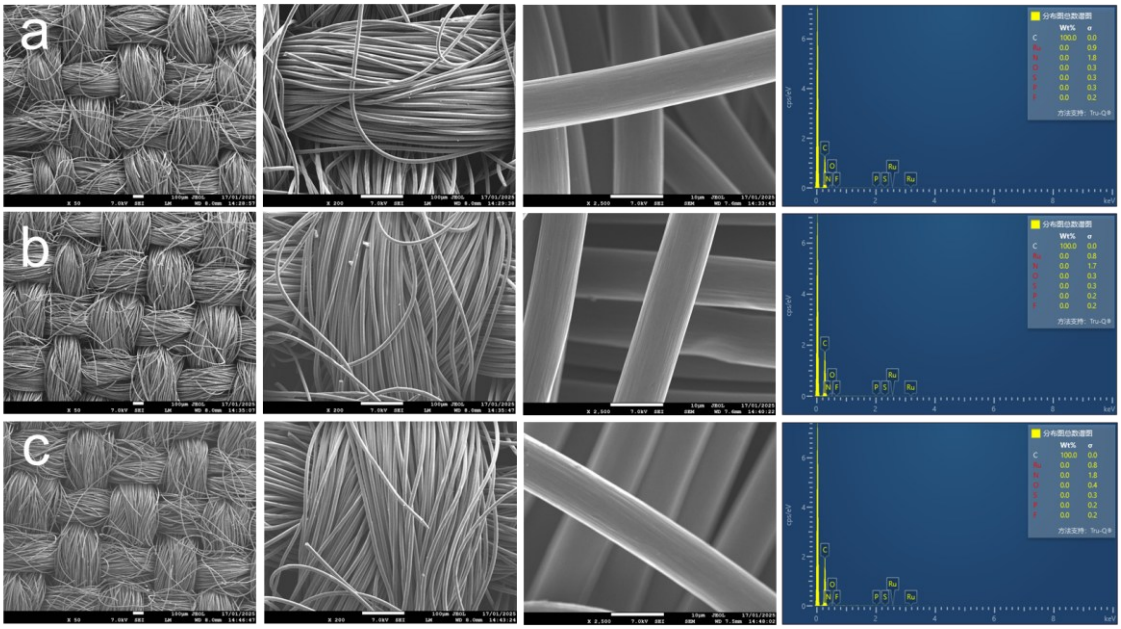

Fig. S43 | SEM images of CC. (a) before; (b) after electrolysis of NH_3 (2.0 M) in presence of **1-NH$_3$** (0.01 mM) in CH_3CN solution under Ar atmosphere at applied potential of 0.8 V vs. $Cp_2Fe^{+/0}$ for 2 h under natural light; (c) the washed CC after electrolysis. The scales of the first three SEM images in a, b, c represent 400, 100, 10μm, respectively.

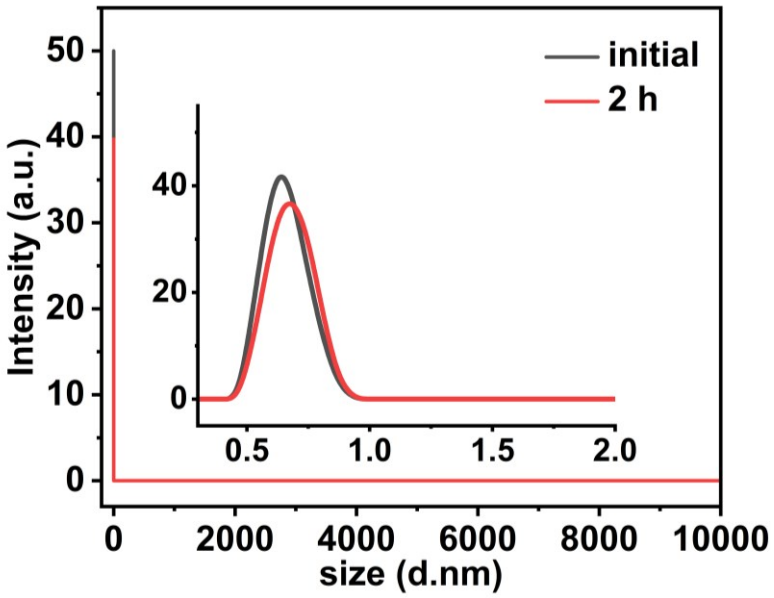

Fig. S44 | DLS curves of (black) before and (red) after CPC experiments by **1-NH$_3$** at E_{app} 0.8 V vs. $Cp_2Fe^{+/0}$ for 2 h under natural light.